Int. J. Heat Mass Transfer. Vol. 31, No. 8, pp. 1723–1734, 1988
Printed in Great Britain

0017–9310/88 $3.00 + 0.00

Characteristics of a turbulent natural convection boundary layer along a vertical flat plate

T. TSUJI and Y. NAGANO

Department of Mechanical Engineering, Nagoya Institute of Technology, Gokiso-cho, Showa-ku, Nagoya 466, Japan

(*Received* 30 *October* 1987 *and in final form* 11 *December* 1987)

Abstract—A detailed hot-wire measurement of a turbulent natural convection boundary layer is made paying close attention to the characteristics of the near-wall region which has not been clarified quantitatively. Heat transfer rate and wall shear stress are determined from mean temperature and mean velocity profiles on theoretical grounds. These measurements yield important results concerning the availability of the conventional analogy between heat and momentum transfer and the concept of the viscous sublayer for natural convection. Also, the streamwise development of the turbulent boundary layer is systematically investigated for mean velocity, mean temperature and both velocity and temperature fluctuations.

1. INTRODUCTION

THE STUDY of the turbulent natural convection boundary layer along a vertical flat plate is one of the principal research themes aimed to clarify the basic structure of turbulent heat transfer phenomena. Turbulent natural convection was a key focus for the attention of researchers around 1970, and much experimental research was carried out at the time. Experiments of the turbulent boundary layer in air were conducted by Warner and Arpaci [1], Cheesewright [2] and Pirovano *et al.* [3]. Lock and Trotter [4], Vliet and Liu [5], Coutanceau [6], Fujii *et al.* [7] and Kutateladze *et al.* [8] carried out experiments in liquid. This spectrum of research treated mainly overall characteristics such as heat transfer, mean temperature and mean velocity profiles. Although there are a few descriptions in the literature with respect to the turbulent quantities [4, 5, 8], the systematic measurement of the turbulent structure was pioneered by Smith [9] in air. Many experiments have since been conducted by Papailiou and Lykoudis [10] in liquid metal, Cheesewright and Doan [11], Miyamoto and Okayama [12], Miyamoto *et al.* [13] and Cheesewright and Ierokipiotis [14, 15] in air, and Bill and Gebhart [16] and Kitamura *et al.* [17] in water. There has thus been remarkable progress in the study of natural-convection turbulent structure.

However, there are many contradictions in the recent research, and universal knowledge has yet to be obtained. These originate in the great difficulty of obtaining reliable measurements, because the turbulent natural convection boundary layer is a flow with relatively large fluctuations of velocity and temperature at low velocity. Measurements of turbulent quantities near the wall are especially difficult, so the turbulent structure has not been elucidated. Also, because the measured result of natural convection is easily influenced by the condition of the experimental apparatus, the remarkable differences among investigative results are encountered even in the most basic measurement of the heat transfer rate. On the other hand, numerical analyses of natural convection using turbulence models have been developed by Smith [9], Mason and Seban [18], Plumb and Kennedy [19], Fujii and Fujii [20], and To and Humphrey [21]. However, the models of these calculations are based for the most part on the research results for forced convection. Thus, the accumulation of a body of reliable measured data related to natural convection is eagerly awaited.

The purpose of this study is to show measured data of the turbulent natural convection boundary layer in air along a vertical plate with high reliability and to clarify the basic characteristics quantitatively. At first, heat transfer rate and wall shear stress, which are important characteristic values, are obtained by measuring mean temperature and mean velocity profiles near the wall, and the concept of the viscous sublayer and the overall analogy between the velocity field and the thermal field near the wall are discussed. Then, using these values, the measurements of mean velocity, mean temperature, intensities of velocity and temperature fluctuations and cross-correlation between velocity and temperature fluctuations are obtained, followed by systematic clarification of how each distribution changes in the direction of the plate height.

2. EXPERIMENTAL APPARATUS AND PROCEDURE

2.1. *Experimental apparatus*

An outline of the experimental apparatus is shown in Fig. 1. The flat surface generating flow was a copper plate 4 m high, 1 m wide and 2 mm thick. To prevent heat distortion of the flatness of the heated surface, the upper end of the plate was suspended by

NOMENCLATURE

c_p specific heat at constant pressure
Gr_x local Grashof number, $g\beta\Delta T_w x^3/\nu^2$
Gr_x^* modified local Grashof number, $g\beta q_w x^4/\lambda\nu^2$
g gravitational acceleration
h heat transfer coefficient
Nu_x local Nusselt number, hx/λ
Pr Prandtl number, $\mu c_p/\lambda$
q_w wall heat flux
R_{ut} cross-correlation coefficient between u and t
T mean fluid temperature
T^+ dimensionless temperature, $(T_w-T)/t_*$
ΔT_w temperature difference, T_w-T_∞
t temperature fluctuation
t_* friction temperature, $q_w/\rho c_p u_*$
U mean streamwise velocity
U_b reference velocity, $(g\beta\Delta T_w\nu)^{1/3}$
U_m maximum velocity along the flat plate
U^+ dimensionless velocity, U/u_*
u streamwise velocity fluctuation
u_* friction velocity, $\sqrt{(\tau_w/\rho)}$
x distance from the leading edge of the flat plate
y distance perpendicular to the flat plate
y^+ dimensionless distance from wall, $u_* y/\nu$.

Greek symbols
α thermal diffusivity
β coefficient of volume expansion, $1/T_\infty$
ζ dimensionless transverse coordinate, $-y(\partial\theta/\partial y)_{y=0}$
θ dimensionless temperature, $(T-T_\infty)/\Delta T_w$
λ thermal conductivity
μ viscosity
ν kinematic viscosity
ρ density
τ_w wall shear stress.

Superscript
$\bar{}$ time averaged quantities.

Subscripts
f film temperature
w wall condition
∞ ambient condition.

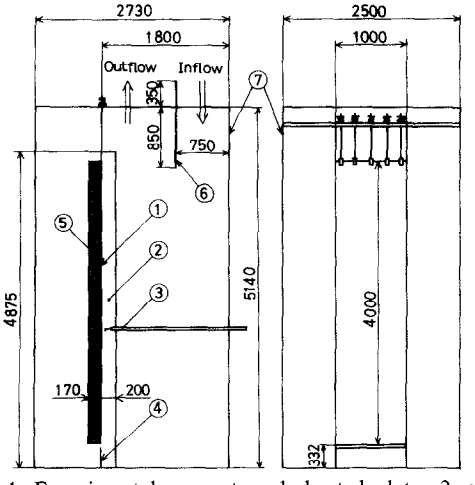

FIG. 1. Experimental apparatus: 1, heated plate; 2, side board; 3, probe; 4, bakelite board; 5, glass wool; 6, partition board; 7, inner wall.

springs. The plate was surrounded with a 2.73, 2.5 and 5.14 m high inner wall of plywood boards, as seen in the same figure, to avoid external turbulence in the room affecting development of the boundary layer.

To heat the plate, stainless-steel strip heaters 15 mm wide and 0.03 mm thick were horizontally attached at 18 mm intervals to the back side of the plate. A uniform surface temperature was obtained by dividing the total 221 stainless-steel strip heaters into 13 units and controlling the heating current of each. Glass wool insulation 170 mm thick was used to reduce heat loss from the back of the plate.

The leading edge of the plate was chamfered to a sharp edge with a 60° angle, and a bakelite board was installed at 7 mm intervals below the edge as shown in Fig. 2. In the case without this board, a swirling flow was introduced near the leading edge of the heated surface due to approaching flow, and a stable laminar boundary layer was not formed. With the configuration as in Fig. 2, a well-defined boundary layer developing from the leading edge was observed by smoke-trace visualization.

Although ascending flow in the natural convection boundary layer was supplied mainly by the entrainment of fluid at the outer edge of the boundary layer, the sidewise entrainment toward the center from both sides of the plate caused decreasing two-dimensionality of the boundary layer. To prevent this effect,

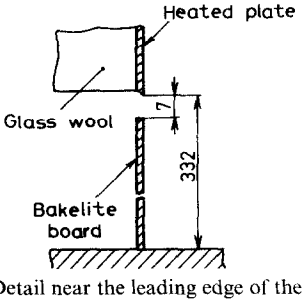

FIG. 2. Detail near the leading edge of the plate.

200 mm wide side boards made of acrylates were set up on both sides of the plate, as seen in Fig. 1, in terms of turbulent boundary layer thickness.

When the flow condition in the inner wall was observed using smoke, the flow was disturbed at the upper part of the heated surface by the interference between ascending flow along the plate and descending flow supplied from the outside of the inner wall. Therefore, a partition board was set up at the upper part of the inner wall as shown in Fig. 1. Its size and location were arranged so that a fine flow field was obtained over the heated surface.

2.2. *Measurements of velocity and temperature*

A normal hot wire and a cold wire made of 3.1 μm diameter tungsten were used to measure fluid velocity and temperature. The lengths of the wires were 1.5 and 3.5 mm, respectively, and the cold wire was located 2.5 mm upstream of the hot wire. Temperature compensation of the hot wire was carried out by the technique of ref. [22]. It was confirmed that there was no interference of the velocity and thermal fields between the two wires. Special attention was paid to the spatial difference between the thermal fields which the hot wire and the cold wire perceived, because of the hot-wire measurement at low velocities. By investigating the spatial difference between the thermal fields at hot- and cold-wire locations, the space correlation coefficient between temperature fluctuations was found to be about 0.98. Although this value approached unity, an error not to be ignored in the measurement of fluctuating velocity was introduced. Therefore, after it was confirmed that Taylor's hypothesis held comparatively well also for the thermal field of the natural convection boundary layer, temperature compensation was performed more precisely by delaying temperature signals of the cold wire. A low-velocity wind tunnel, shown in ref. [23], was used for the velocity calibration of the hot wire.

A 0.025 mm diameter platinum–rhodium–platinum thermocouple was used simultaneously for the measurement of fluid temperature near the wall, and precise heat transfer coefficients were obtained. The thermocouple was set onto the prongs (i.e. support needles) 15 mm apart. Thus, the length of the thermocouple was 600 times the diameter, and the measurement error produced by the difference between prong temperature and fluid temperature could be ignored in this case.

These measuring probes, connected to a traveling microscope established at the outside of the inner wall, were traversed at the center-line on the heated surface. With respect to the two-dimensionality of the boundary layer, it was confirmed previously from the measurement of the thermal field that the distributions of mean temperature T and temperature fluctuation t were uniform in the direction of plate width.

In the turbulent boundary layer and the transition region, temperature and velocity fluctuated highly irregularly. Measured data were recorded with a data-recorder for 1–5 min and were processed with a computer (FACOM-M382) after analog to digital conversion at a sampling frequency of 400 Hz.

Ambient fluid temperature T_∞ was measured with seven thermocouples placed over the 4.5 m height 600 mm away from the heated surface. The surface temperature T_w was measured with 0.1 mm diameter copper–constantan thermocouples embedded in the back of the plate. The measuring positions were 21 points along the center-line of the plate and 5 points each along either side-line 350 mm apart from the center-line.

2.3. *Experimental conditions*

Experiments were carried out at a uniform surface temperature of 60°C. Measurements of heat transfer rate were also affected at a surface temperature of 100°C. Ambient fluid temperature was about 16°C at a height of 2 m from the leading edge of the plate and increased nearly 2°C in the height direction from the leading to the trailing edges of the plate.

Physical properties were evaluated at the film temperature $T_f = (T_w + T_\infty)/2$, except that the body expansion coefficient β was defined as $1/T_\infty$. In comparison between measured values and theoretical ones, physical properties were strictly evaluated in the same manner as the theory.

3. LAMINAR BOUNDARY LAYER

The results of velocity and temperature measurements in the laminar boundary layer are shown in Fig. 3. The solid lines indicate the theoretical solutions to laminar boundary layer equations with variable properties that were calculated to make a close comparison with experiments. The theoretical solutions were obtained with the variables based on ambient fluid temperature. In terms of the ease of comparison with experimental values, these solutions have advantages over those by Sparrow and Gregg [24] (Cairnie and Harrison [25]). Agreement between the theor-

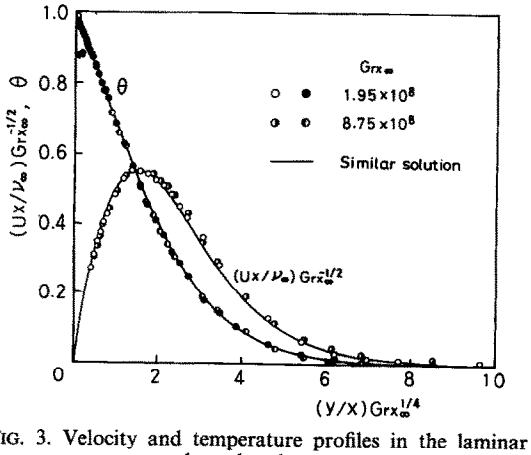

FIG. 3. Velocity and temperature profiles in the laminar boundary layer.

etical values and measurements is excellent for both mean velocity and mean temperature profiles. This result shows that the stable boundary layer developed from the leading edge of the heated surface, and the measuring method was adequate for the present experiment.

4. HEAT TRANSFER RATE

The wall heat flux q_w necessary to estimate the heat transfer coefficient $h = q_w/\Delta T_w$ was obtained from $-\lambda_w(\partial T/\partial y)_{y=0}$. An example of mean temperature profiles near the wall in the turbulent boundary layer, which were used to determine q_w, is presented in Fig. 4 in the form of θ. The turbulent boundary layer was obtained in the range $Gr_x > 10^{10}$ as described presently. Although the mean temperature profiles shown in Fig. 4 were obtained using a thermocouple, there was no significant difference between this result and that using the cold wire. It is evident from the figure that the mean temperature profiles are linear in the range of $y < 2$ mm. However, to improve accuracy, the wall heat flux q_w was estimated mainly from the mean temperature profile in the very near-wall region $y \leqslant 0.5$ mm.

The experimental result of heat transfer rates is shown in Fig. 5 in the relation between Nusselt number Nu_x and Rayleigh number $Gr_x Pr$. For the heat transfer rate, measurements at a surface temperature of 100°C are drawn together. Although the wall heat flux was assessed from the fluid temperature gradient near the wall in the present experiment, almost the same result was obtained also from deducting heat loss from electric power consumption for heating the plate. But the measurement with the temperature gradient was more accurate, and the local wall heat flux could be obtained precisely.

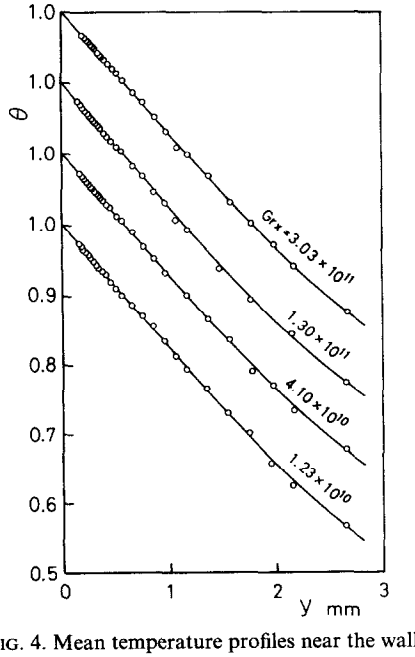

FIG. 4. Mean temperature profiles near the wall.

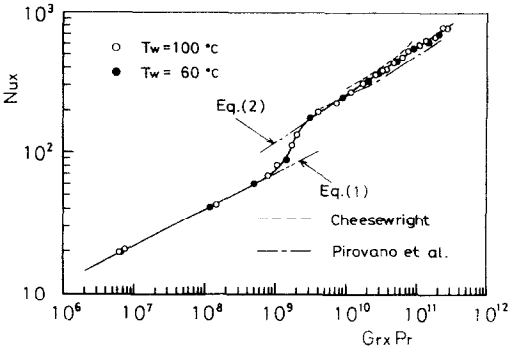

FIG. 5. Heat transfer rates.

In the laminar boundary layer, the following theoretical equation agrees very well with experimental values:

$$Nu_x = 0.387(Gr_x Pr)^{1/4}. \quad (1)$$

At $Gr_x Pr = 8 \times 10^8$, Nu_x begins to deviate from the theoretical value of the laminar boundary layer.

In the present experiment, heat transfer rates were measured up to $Gr_x Pr = 3 \times 10^{11}$. Heat transfer rates in the turbulent boundary layer are expressed well by the following empirical formula:

$$Nu_x = 0.120(Gr_x Pr)^{1/3}. \quad (2)$$

Equation (2) holds in the range $Gr_x Pr > 3.5 \times 10^9$. However, the developed turbulent boundary layer cannot be obtained until about $Gr_x Pr > 7 \times 10^9$, as described later, judging by the mean velocity and mean temperature profiles in the boundary layer.

For comparison, the measurements in the turbulent region of Cheesewright [2, 26] and Pirovano *et al.* [3], which were conducted under the condition of uniform surface temperature, are also shown in the figure. The present experimental values range in between both results and are well correlated with equation (2). Although not shown in the figure, the measurement of Smith [9] (in whose experiment the surface temperature was not uniform and the temperature difference between the surface and ambient fluid was kept constant in the plate height direction) was slightly lower than the result of Cheesewright [2, 26]. The measurements of Warner and Arpaci [1] and Warner [27] are lower than those of Pirovano *et al.* [3]. Although Cheesewright [2, 26] and Pirovano *et al.* [3] gave a local increase of Nu_x near the commencement of the turbulent boundary layer, such an increase of Nu_x was not so obvious in the present experiment. This trend also did not appear in the measurements of Warner and Arpaci [1] or Warner [27]. Miyamoto and Okayama [12], who supposed a uniform wall heat flux, gave heat transfer rates in between those of the present experiment and the result of Cheesewright [2, 26]. They also indicated that there was a local increase of Nu_x only under the high heat flux condition.

It is conceivable that the experimental apparatus used in fact exerted a considerable influence in creating the discrepancy between these results. In the present experiment, the apparatus was devised so that the change of ambient fluid temperature in the plate height direction would be as small as possible, paying attention to the entrainment condition of ambient fluid outside the boundary layer. The increase of ambient fluid temperature in the plate height direction was about 0.5–0.7°C m^{-1} in the range of the turbulent boundary layer. Although the details of the entrainment condition of ambient fluid are unclear as to other measurements, the increase of ambient fluid temperature in the plate height direction was about 1.8°C m^{-1} in the measurement of Cheesewright [2, 26], while that in the measurement of Pirovano *et al.* [3] was only about 0.2°C m^{-1} because the space (including the heated surface) was very large. On the other hand, the temperature increase was about 1.3°C m^{-1} in the measurement of Smith [9], 1.2–1.5°C m^{-1} according to Warner [27] and about 1.6°C m^{-1} (changing considerably in terms of the magnitude of the wall heat flux) in the measurement of Miyamoto and Okayama [12]. When the relation between the difference of experimental conditions and the discrepancy of Nu_x distributions is investigated, it may be said that Nu_x generally tends to be large, as the increase of ambient fluid temperature in the plate height direction becomes large, in the case that heat transfer rates are expressed in the relation between Nu_x and $Gr_x Pr$. The increase of Nu_x with increasing ambient fluid temperature appears even in the theoretical analysis of the laminar boundary layer [26, 28] as well as the calculation for the turbulent boundary layer [15]. Values of Nu_x obtained by Warner and Arpaci [1] and Warner [27] are exceptionally smaller. The cause of this discrepancy is not clear.

The heat transfer characteristic in the transition region has not been clarified by the results of Cheesewright [2, 26] or Pirovano *et al.* [3]. Judging from the present experiment, there is not much difference in the relation between Nu_x and $Gr_x Pr$ for the transition region for the surface temperature conditions of 100 and 60°C.

5. WALL SHEAR STRESS

For measuring wall shear stress precisely, reliable data of the mean velocity profile near the wall are necessary. Figure 6 shows the profiles of mean velocity U near the wall in the turbulent boundary layer. In the velocity measurement with a hot wire, the measured velocity near the wall is greater than the true value. This difference is due to the distortion in the velocity and thermal fields around the hot wire by the wall-proximity effects [29–32]. Also shown in Fig. 6 are modified velocities which were obtained by correcting the measured values. The corrective heat transfer coefficient Δh_c of the hot wire for the wall-proximity effects was obtained by comparing the measured value

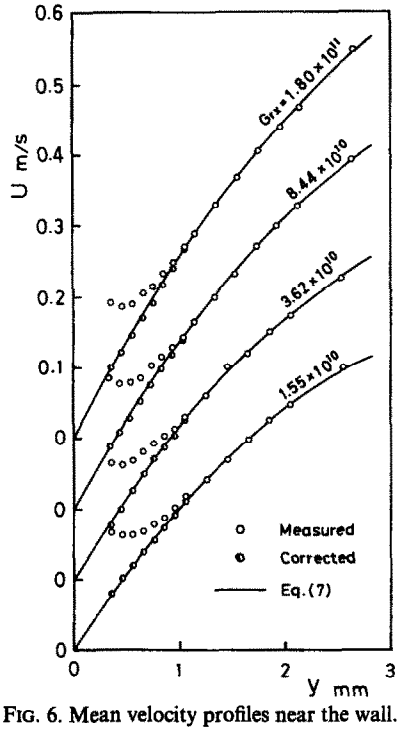

FIG. 6. Mean velocity profiles near the wall.

(measurements subject to wall-proximity effects are omitted in Fig. 3) and the theoretical one in the laminar boundary layer, supposing Δh_c as a function only of the distance y from the wall. However, it is necessary to determine whether this correction is appropriate and the estimation of wall shear stress based on this result is accurate. Therefore, in the present study, wall shear stress was obtained by the method described below on the basis of theoretical consideration.

Near the wall, thermal energy and momentum equations can be described approximately as follows:

$$\frac{\partial}{\partial y}\left(\alpha\frac{\partial T}{\partial y}-\overline{vt}\right)=0 \tag{3}$$

$$\frac{\partial}{\partial y}\left(\nu\frac{\partial U}{\partial y}-\overline{uv}\right)+g\beta(T-T_\infty)=0. \tag{4}$$

By expanding $\overline{vt}$ in series and integrating equation (3) we obtain

$$T=T_w-\frac{q_w}{\lambda}y+\frac{1}{\alpha}\left\{\frac{1}{4!}\left(\frac{\partial^3\overline{vt}}{\partial y^3}\right)_{y=0}y^4+\ldots\right\}. \tag{5}$$

From equation (5), it is found that the contribution of fluctuating components is of the order of more than y^4 and the mean temperature profile near the wall displays straight-line agreement with the experimental result.

Similarly, by expanding $\overline{uv}$ in series and integrating equation (4) with equation (5) for the temperature profile we obtain

$$U=\frac{\tau_w}{\mu}y-\frac{1}{2!}\frac{g\beta\Delta T_w}{\nu}y^2+\frac{1}{3!}\frac{g\beta q_w}{\lambda\nu}y^3+\frac{1}{\nu}\left\{\frac{1}{4!}\left(\frac{\partial^3\overline{uv}}{\partial y^3}\right)_{y=0}y^4+\ldots\right\}. \quad (6)$$

As understood from equation (6), the contribution of fluctuating components appears of the order of more than y^4, and the influence of $\overline{uv}$ is obviously very small near the wall. Therefore, the following equation, neglecting the $\overline{uv}$ term in equation (4), was used for the estimation of wall shear stress:

$$U=\int_0^y\left[\left\{\tau_w-\int_0^{y'}\rho g\beta(T-T_\infty)\,dy'\right\}\Big/\mu\right]dy. \quad (7)$$

Since the temperature change near the wall was large, variations of density ρ and viscosity μ were taken into consideration in order to increase the accuracy. The wall shear stress τ_w was determined so that equation (7) best coincided with the mean velocity profile in the region 1 mm $< y <$ 2 mm, where hot-wire output was not affected by wall proximity. The solid lines shown in Fig. 6 express equation (7) and agree extremely well with the measured values in this range. The measurements for $y <$ 1 mm, corrected for the wall-proximity effects, also agree very well with equation (7). Thus, in natural convection of low velocity, the correct mean velocity profile can be obtained by adding the same correction just as for the laminar boundary layer to the measurements for the turbulent boundary layer. However, this correction is not valid in general for high Reynolds number flows [29].

Since the buoyancy terms of y^2 and y^3, as seen in equation (6), do not appear in the forced-convection velocity profile near the wall, it is well known that there exists a linear region $U^+=y^+$ in the viscous sublayer adjacent to the wall, say $y^+ \leqslant 5$. In natural convection, however, Lock and Trotter [4, 33] doubted the existence of any viscous sublayer from their observation of temperature fluctuation near the wall. Kutateladze *et al.* [8] concluded that the linear region did not exist near the wall from the form of the integral equation (7). On the other hand, Plumb and Kennedy [19] and George and Capp [34] suggested the existence of a linear region near the wall from considering a series expanded equation of the mean velocity profile with y, as shown by equation (6). These confusions originate from the fact that the precise mean velocity profile near the wall has not been measured and the reliable value of wall shear stress cannot be estimated.

When each term in equation (6) is evaluated using the values of wall shear stress and wall heat flux estimated in the present study, it is found in the case $Gr_x=8.44\times10^{10}$ shown in Fig. 6 that the y^2 term is about 15% of the y term and the y^3 term is about 0.9% of the y term at the location of $y=1$ mm (equivalent to $y^+=4.1$). Eventually, in the turbulent natural convection boundary layer, the mean velocity profile approaches a straight-line in the region much nearer the wall ($y^+<1$), and it seems difficult to maintain the same concept of the viscous sublayer as for forced convection. This is one of the important results obtained in the present study as a notable characteristic of natural convection.

The distribution of wall shear stresses τ_w is shown in Fig. 7. When the theoretical value of τ_w for the laminar boundary layer is calculated with variable properties, the following equation is obtained:

$$\tau_w/\rho U_b^2=0.953Gr_x^{1/12} \quad (8)$$

where U_b is a reference velocity (defined as $(g\beta\Delta T_w\nu)^{1/3}$). As seen in Fig. 7, the measured values agree very well with the above theoretical equation.

On the other hand, the experimental result for the turbulent boundary layer is very well correlated with the following equation:

$$\tau_w/\rho U_b^2=0.684Gr_x^{1/11.9}. \quad (9)$$

Obviously, the index of Gr_x is very close to that in the laminar boundary layer.† The streamwise variation of wall shear stress produced in natural convection is the complete opposite of that for the plane boundary layer flow of forced convection. The wall shear stress τ_w increases with increasing Gr_x for the laminar and turbulent boundary layers and decreases in the transition region. In the natural convection boundary layer, the heat transfer coefficient h shown previously is almost constant, whereas the wall shear stress increases with increasing Gr_x. Therefore, the analogy between heat and momentum transfer does not hold, which is in marked contrast to that observed in the usual turbulent boundary layer.

The results of Smith [9] and Cheesewright and Ierokipiotis [15] are also shown in Fig. 7 by the broken line and the chain line, respectively. Both groups estimated the wall shear stress τ_w, assuming that the measured mean velocity profile complied with the third-order polynomial expression of the distance y from the wall. In the hot-wire measurement of Smith [9], the velocity

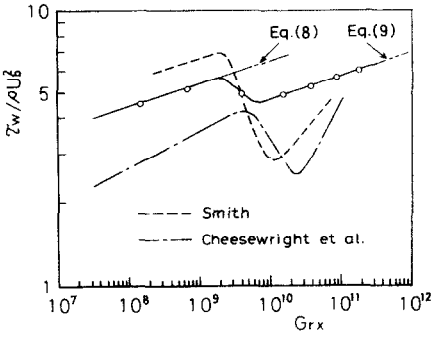

FIG. 7. Wall shear stresses.

† Although equation (9) is obtained by least squares regression analysis, there is almost no difference for $\tau_w/\rho U_b^2=0.696Gr_x^{1/12}$.

near the wall was not enough to obtain τ_w, and the uncertainty interval [35] estimated for the measurement was also considerably large. The LDV measurement of Cheesewright and Ierokipiotis [15] seems to be insufficiently accurate to estimate the correct τ_w (with volume at about 0.6 mm, precise measurement in the near-wall region $y < 2$ mm, where the velocity gradient is sharp, could not be expected). Both measured results clearly disagreed with the theoretical value for the laminar region.

6. MEAN VELOCITY AND MEAN TEMPERATURE PROFILES IN THE TURBULENT BOUNDARY LAYER

6.1. *Mean velocity profile*

Mean velocity profiles for the turbulent boundary layer, normalized by the friction velocity u_*, are shown in Fig. 8 in the relation between U^+ and y^+. For comparison, velocity profiles for the transition and laminar regions are indicated by the dot chain line and the two-dot chain line, respectively. Velocity profiles for the turbulent boundary layer depend on Gr_x, although they have a similar form. In the turbulent forced convection boundary layer, it is well known that the following mean velocity profile holds for the viscous sublayer of $y^+ \leqslant 5$:

$$U^+ = y^+. \tag{10}$$

In the turbulent natural convection boundary layer, the effect of the buoyancy terms appears in the velocity profile as previously expressed by equation (6), so that equation (10) does not hold even at $y^+ \simeq 1$. The maximum velocity location y_m corresponds to $y_m^+ \simeq 30$–40 as the minimum and the y_m value increases with increasing Gr_x. The logarithmic velocity profile that appears in the region $y^+ > 30$ in the usual turbulent forced convection boundary layer, cannot be seen at all. The turbulent characteristics of the velocity fields bordering the maximum velocity location are fairly different, as will be shown later. Therefore, after Townsend [36], we refer to the region from the maximum velocity location y_m to the edge of the boundary layer as the outer layer and the region between y_m and the heated surface as the inner layer. The inner layer thickness is about 1/20 of the boundary layer thickness.

A comparison of mean velocity profiles obtained in the present experiment and measurements of other researchers [9, 13, 14] is shown in Fig. 9. The velocity U is normalized by the maximum value U_m, and the coordinate ζ is defined by the following equation:

$$\zeta = -y(\partial\theta/\partial y)_{y=0}. \tag{11}$$

This variable ζ was used for correlating the mean temperature profiles for turbulent boundary layers in spindle oil and water by Fujii *et al.* [7]. Because the streamwise variation of the wall heat flux in the turbulent boundary layer is very small even with uniform surface temperature, the coordinate ζ is almost in proportion to y alone. Accordingly, the mean velocity profiles shown in Fig. 8 cannot be determined in these coordinates, even if they are rearranged (as with the measurements of Miyamoto *et al.* [13]). However, the coordinates have been well used conventionally for the arrangement of mean temperature profiles. All measurements roughly agree for the inner layer extending from the wall vicinity to the maximum location. In the outer layer, however, other measured results become smaller than the present ones and show a thinner boundary layer. This indicates that the increase in ambient temperature in the plate height direction in any other experiment was greater than in the present one as mentioned before, and so the development of the boundary layer is restrained.

6.2. *Mean temperature profile*

Mean temperature profiles are presented in Fig. 10 in the relation between T^+ and y^+. Temperature profiles for the transition region and laminar boundary layer are also indicated in the figure for comparison by the dot chain line and the two-dot chain line, respectively. Since the mean temperature profile becomes almost a straight-line as the wall is approached, it is well described with the following

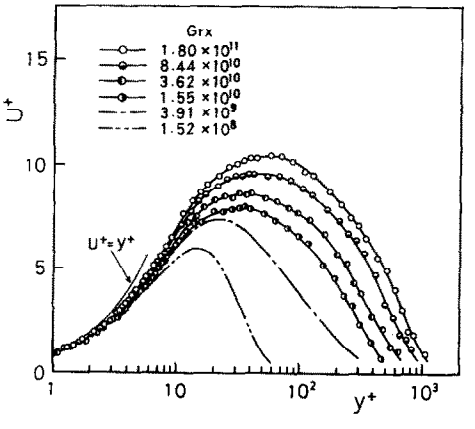

FIG. 8. Mean velocity profiles.

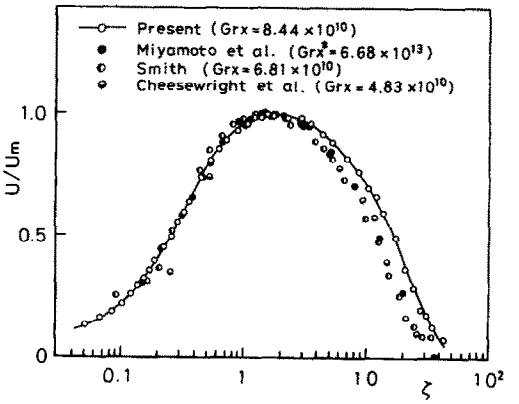

FIG. 9. Comparison of mean velocity profiles.

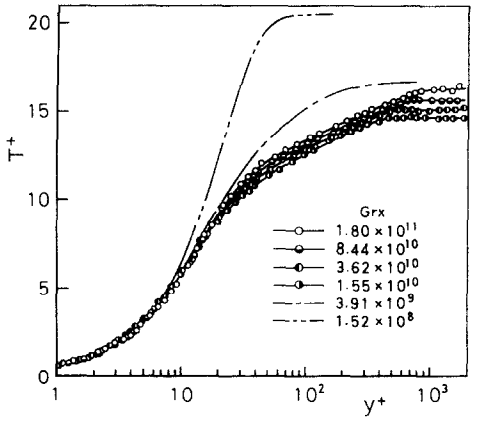

FIG. 10. Mean temperature profiles.

equation in the region $y^+ \leqslant 5$, similar to that for the forced convection boundary layer:

$$T^+ = Pr\, y^+. \tag{12}$$

The mean temperature profile in the region $y^+ > 5$ varies with the development of the boundary layer in the same manner as the mean velocity profile. In the region $30 \leqslant y^+ \leqslant 200$, a logarithmic temperature profile expressed by the following equation appears as in forced convection:

$$T^+ = (1/\kappa_t) \ln y^+ + C \tag{13}$$

where constant C varies with increasing Gr_x, and κ_t is almost a universal constant of 0.69.

A comparison of the present mean temperature profile with other measurements [9, 26, 37] is shown in Fig. 11 in the relation between θ and ζ. If these coordinates are used, the mean temperature profiles shown in Fig. 10 are well correlated in the inner layer ($\zeta < 1.5$). However, in the outer layer, the profiles depend on Gr_x and cannot be determined after all. Although other measurements are also correlated in the inner layer and almost agree with the present result, the thermal boundary layers become thinner than in the present experiment due to the large temperature change in the ambient fluid.

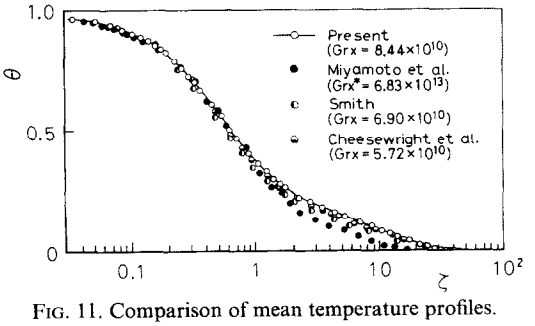

FIG. 11. Comparison of mean temperature profiles.

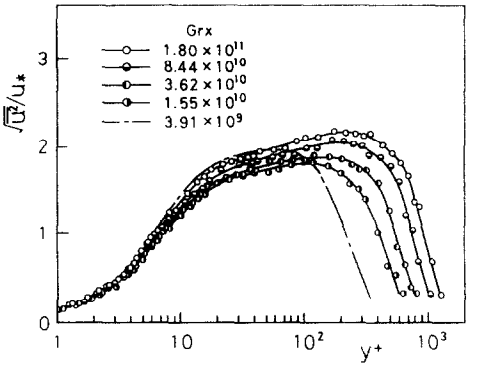

FIG. 12. Intensity distributions of velocity fluctuation.

7. VELOCITY AND TEMPERATURE FLUCTUATIONS

7.1. *Intensity of velocity fluctuation*

The distributions of streamwise velocity fluctuation intensity normalized by the friction velocity u_* are presented as a function of y^+ in Fig. 12. Although the measurements near the wall (below $y^+ \simeq 4$) may receive the wall-proximity effects, no correction is made. When normalizing the measured values in the range from the wall vicinity to the maximum velocity location by local mean velocity U, a constant value $\sqrt{(\overline{u^2})}/U \simeq 0.20$ is obtained regardless of Gr_x (figure omitted). Therefore, in the inner layer, the variation of the intensity of velocity fluctuation with Gr_x corresponds well to that of the mean velocity with Gr_x. This relative intensity, $\sqrt{(\overline{u^2})}/U \simeq 0.20$, is comparatively close to $\sqrt{(\overline{u^2})}/U \simeq 0.25$ [38] and 0.23 [39] observed near the wall in forced convection. The maximum intensity of the velocity fluctuation occurs in the outer layer ($y^+ \simeq 100$–300). In Fig. 12, the distribution of velocity fluctuation intensity in the transition region is also given by the chain line for comparison. Obviously, the maximum intensity of velocity fluctuation increases rapidly in the transition region and, after once decreasing at the commencement of the turbulent boundary layer, it increases again with the development of the boundary layer. This behavior is also seen in the measurement of Smith [9].

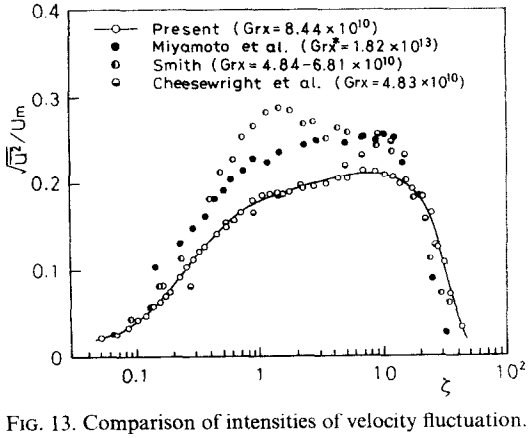

FIG. 13. Comparison of intensities of velocity fluctuation.

A comparison of the intensity of the velocity fluctuation with other measurements is shown in Fig. 13 in the relation between $\sqrt{(\overline{u^2})}/U_m$ and ζ. The result obtained using the LDV of Cheesewright and Ierokipiotis [14] generally agrees well with the present result, although there is a somewhat large value in the vicinity of the maximum intensity location. Miyamoto *et al.* [13], who also used an LDV, obtained results similar to the present ones, but they became larger in the range from the inner layer to part of the outer layer. The quantitative discrepancy with the present result is attributed to the difference in experimental conditions such as the upward change of ambient fluid temperature and the entrainment of ambient fluid to the boundary layer. In fact, the development of the maximum velocity with Gr_x in the experiment of Miyamoto *et al.* [13] becomes relatively very small in comparison with the variation of the maximum intensity of velocity fluctuation with Gr_x. On the other hand, the measured result using the hot wire of Smith [9] assumes maximum intensity near the maximum velocity location ($\zeta \simeq 1.5$) and shows a tendency different from other results. It is thought that an error resulted in the measurement of velocity fluctuation in the range of large temperature fluctuation, as mentioned later, due to the spatial difference between the thermal fields around the hot wire and thermocouple used for temperature compensation and also owing to the different frequency responses of the hot wire and the thermocouple.

7.2. *Intensity of temperature fluctuation*

The distributions of temperature fluctuation intensity normalized by the friction temperature t_* are shown as a function of y^+ in Fig. 14. The temperature fluctuation becomes maximum at $y^+ \simeq 15$ in the inner layer. Near the wall $y^+ < 15$, the measured values are well correlated in the same manner as the mean temperature profile (Fig. 10). Because the velocity fluctuation becomes maximum in the outer layer, the locations of the maximum velocity fluctuation and the maximum temperature fluctuation are fairly far apart. On the contrary, in forced convection (air flow), both fluctuations of velocity and temperature take the maximum values in the inner layer near the wall [39, 40]. Therefore, the characteristics of velocity and temperature fluctuations in natural convection are also remarkably different from those in forced convection. The chain line indicated in Fig. 14 is the measured result for the transition region. The intensity of temperature fluctuation increases rapidly in the transition region and decreases at the commencement of the turbulent boundary layer, similar to the intensity of the velocity fluctuation.

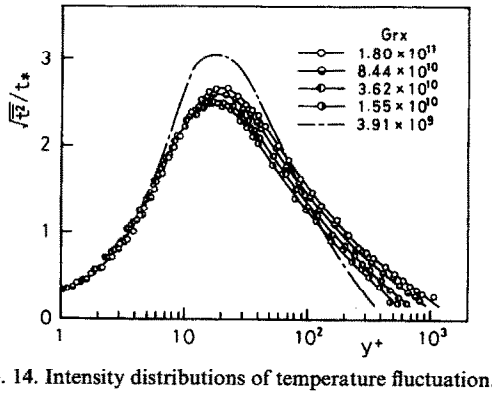

FIG. 14. Intensity distributions of temperature fluctuation.

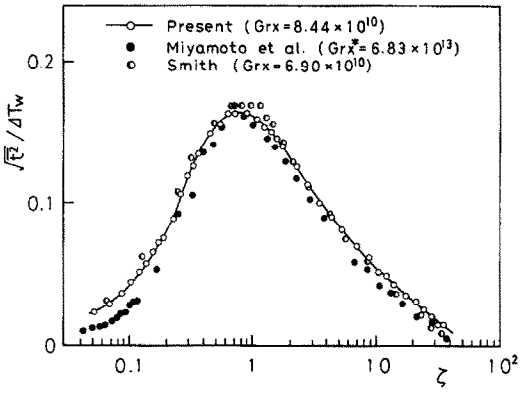

FIG. 15. Comparison of intensities of temperature fluctuation.

A comparison of the presently measured intensity of temperature fluctuation with the measurements of other authors, is presented in Fig. 15 in the relation between $\sqrt{(\overline{t^2})}/\Delta T_w$ and ζ. All measurements coincide relatively well, although the result of Miyamoto *et al.* [13] is somewhat small.

7.3. *Cross-correlation between velocity and temperature fluctuations*

The distributions of $\overline{ut}$, the cross-correlation between velocity and temperature fluctuations (i.e. streamwise turbulent heat flux), are presented in Fig. 16. In the region $y^+ \leqslant 5$, $\overline{ut}$ (not being corrected for wall-proximity effects) takes a value of about zero. The ut value increases rapidly in the positive direction near the location of the maximum temperature fluc-

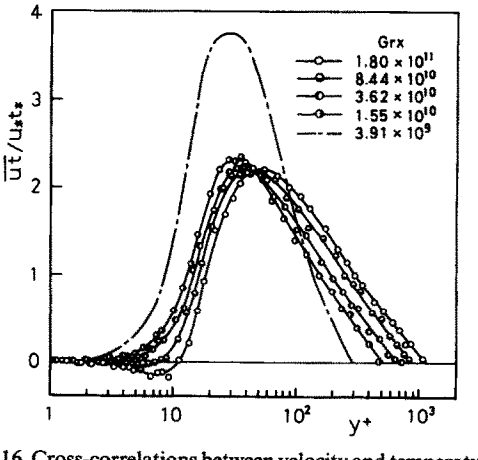

FIG. 16. Cross-correlations between velocity and temperature fluctuations.

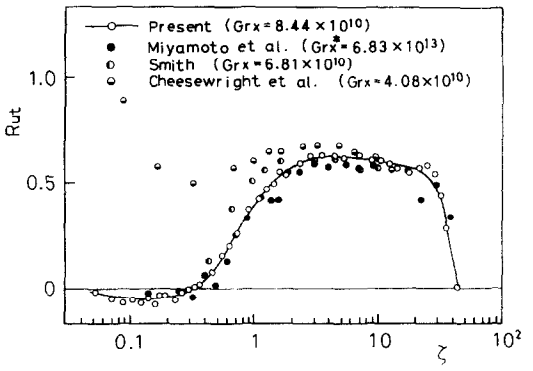

FIG. 17. Comparison of cross-correlation coefficients between velocity and temperature fluctuations.

tuation and reaches a maximum at the location almost equivalent to the maximum velocity location. In the forced convection boundary layer (e.g. a pipe flow [39]), $\overline{ut}$ takes a negative value in the case of heated flow ($\partial U/\partial y > 0$, $\partial T/\partial y < 0$). Also, in natural convection, $\overline{ut}$ near the wall tends to become gradually negative with the development of the boundary layer, as the mean velocity profile approaches the universal velocity profile seen in forced convection. However, the absolute value is far smaller than the corresponding value for forced convection. The result for the transition region is also shown in Fig. 16 by the chain line. In the transition region, the cross-correlation increases rapidly and decreases at the commencement of the turbulent boundary layer in the same manner as other turbulent quantities. However, the variation of the maximum value with the development of the turbulent boundary layer is as small as that of the maximum temperature fluctuation.

The result of $\overline{ut}$ is compared with other measurements in Fig. 17 in the form of the cross-correlation coefficient $R_{ut} = \overline{ut}/\sqrt{(\overline{u^2})}\sqrt{(\overline{t^2})}$. The present result agrees very well with that of Miyamoto *et al.* [13] over the entire boundary layer region. Although Smith [9] and Cheesewright and Doan [11] used the same experimental apparatus and carried out similar hot-wire measurements, they reported contradictory results (i.e. one decreased and the other increased as the wall was approached). In a fairly wide region extending from the maximum velocity location to the outer layer, the differences in all measurements become small and the R_{ut} values tend to agree almost throughout the range of 0.6–0.7.

8. CONCLUSIONS

To clarify the basic characteristics of the turbulent natural convection boundary layer along a vertical flat plate, detailed measurements of the temperature and velocity fields were made paying close attention to experimental conditions such as entrainment of ambient fluid to the boundary layer and the ambient fluid temperature change in the height direction.

Results obtained in the present study may be summarized as follows.

(1) The Nusselt number in the turbulent boundary layer, estimated from measuring the mean temperature profile very near the wall, is described very well by equation (2). The heat transfer rate in the turbulent natural convection boundary layer is largely influenced by the increasing rate of ambient fluid temperature in the plate height direction.

(2) Wall shear stress in the turbulent boundary layer, which was estimated combining a theoretical approach with the precise measurement of the mean velocity profile near the wall, is expressed well by equation (9), and the change of wall shear stress with Gr_x is very close to that in the laminar boundary layer.

(3) Although wall shear stress increases in the plate height direction in the natural convection boundary layer, the heat transfer rate is almost constant. Thus, the analogy between heat and momentum transfer, applied frequently for the near-wall turbulence in the usual boundary layer, does not hold.

(4) On the basis of measurements of heat transfer rate and wall shear stress, the mean velocity, mean temperature, intensities of velocity and temperature fluctuations and cross-correlation between velocity and temperature fluctuations were arranged by the flow parameters for the inner layer similar to forced convection and were shown in comparison with those for forced convection. One of the important results in the natural convection boundary layer is that the mean velocity profile for the turbulent boundary layer approaches a straight-line only in the region of much smaller y^+, and thus the same concept of the viscous sublayer as forced convection seems no longer valid.

(5) For the near-wall measurement, the hot-wire technique used in the present study is more effective and yields better results than the LDV technique, with its disadvantage in measuring volume.

Acknowledgements—The authors wish to express their thanks to Dr M. Hishida for beneficial discussions throughout the present study.

REFERENCES

1. C. Y. Warner and V. S. Arpaci, An experimental investigation of turbulent natural convection in air at low pressure along a vertical heated flat plate, *Int. J. Heat Mass Transfer* **11**, 397–406 (1968).
2. R. Cheesewright, Turbulent natural convection from a vertical plane surface, *J. Heat Transfer* **90**, 1–8 (1968).
3. A. Pirovano, S. Viannay et M. Jannot, Convection naturelle en regime turbulent le long d'une plaque plane verticale, *Proc. 9th Int. Heat Transfer Conf., Natural Convection*, Vol. 4, NC 1.8, pp. 1–12. Elsevier, Amsterdam (1970).
4. G. S. H. Lock and F. J. deB. Trotter, Observations on the structure of a turbulent free convection boundary layer, *Int. J. Heat Mass Transfer* **11**, 1225–1232 (1968).
5. G. C. Vliet and C. K. Liu, An experimental study of turbulent natural convection boundary layers, *J. Heat Transfer* **91**, 517–531 (1969).
6. J. Coutanceau, Convection naturelle turbulente sur une plaque verticale isotherme, transition, echange de chal-

eur et frottement parietal, lois de repartition de vitesse et de temperature, *Int. J. Heat Mass Transfer* **12,** 753–769 (1969).
7. T. Fujii, M. Takeuchi, M. Fujii, K. Suzaki and H. Uehara, Experiments on natural-convection heat transfer from the outer surface of a vertical cylinder to liquids, *Int. J. Heat Mass Transfer* **13,** 753–787 (1970).
8. S. S. Kutateladze, A. G. Kirdyashkin and V. P. Ivakin, Turbulent natural convection on a vertical plate and in a vertical layer, *Int. J. Heat Mass Transfer* **15,** 193–202 (1972).
9. R. R. Smith, Characteristics of turbulence in free convection flow past a vertical plate, Ph.D. Thesis, University of London (1972).
10. D. D. Papailiou and P. S. Lykoudis, Turbulent free convection flow, *Int. J. Heat Mass Transfer* **17,** 161–172 (1974).
11. R. Cheesewright and K. S. Doan, Space–time correlation measurements in a turbulent natural convection boundary layer, *Int. J. Heat Mass Transfer* **21,** 911–921 (1978).
12. M. Miyamoto and M. Okayama, An experimental study of turbulent free convection boundary layer in air along a vertical plate using LDV, *Bull. J.S.M.E.* **25,** 1729–1736 (1982).
13. M. Miyamoto, H. Kajino, J. Kurima and I. Takanami, Development of turbulence characteristics in a vertical free convection boundary layer, *Proc. 7th Int. Heat Transfer Conf.*, Munich, F.R.G., Vol. 2, pp. 323–328 (1982).
14. R. Cheesewright and E. Ierokipiotis, Velocity measurements in a turbulent natural convection boundary layer, *Proc. 7th Int. Heat Transfer Conf.*, Munich, F.R.G., Vol. 2, pp. 305–309 (1982).
15. R. Cheesewright and E. Ierokipiotis, Measurements in a turbulent natural convection boundary layer, *1st U.K. Conf. on Heat Transfer*, Vol. 2, pp. 849–856. I.Chem.E. (1984).
16. R. G. Bill and B. Gebhart, The development of turbulent transport in a vertical natural convection boundary layer, *Int. J. Heat Mass Transfer* **22,** 267–277 (1979).
17. K. Kitamura, M. Koike, I. Fukuoka and T. Saito, Large eddy structure and heat transfer of turbulent natural convection along a vertical flat plate, *Int. J. Heat Mass Transfer* **28,** 837–850 (1985).
18. H. B. Mason and R. A. Seban, Numerical predictions for turbulent free convection from vertical surfaces, *Int. J. Heat Mass Transfer* **17,** 1329–1336 (1974).
19. O. A. Plumb and L. A. Kennedy, Application of a K–ε turbulence model to natural convection from a vertical isothermal surface, *J. Heat Transfer* **99,** 79–85 (1977).
20. T. Fujii and M. Fujii, A numerical analysis on the turbulent free convection (1st report for the case of air), *Trans. Japan Soc. Mech. Engrs* **43,** 3825–3834 (1977).
21. W. M. To and J. A. C. Humphrey, Numerical simulation of buoyant, turbulent flow—1. Free convection along a heated, vertical, flat plate, *Int. J. Heat Mass Transfer* **29,** 573–592 (1986).
22. M. Hishida and Y. Nagano, Simultaneous measurements of velocity and temperature in nonisothermal flows, *J. Heat Transfer* **100,** 340–345 (1978).
23. T. Tsuji, Y. Nagano and H. Fukuoka, Turbulence measurements at low velocities with symmetrically bent V-shaped hot-wires (1st report heat transfer characteristics), *Trans. Japan Soc. Mech. Engrs*, Series B **53,** 413–417 (1987).
24. E. M. Sparrow and J. L. Gregg, The variable fluid-property problem in free convection, *Trans. ASME* **80,** 879–886 (1958).
25. L. R. Cairnie and A. J. Harrison, Natural convection adjacent to a vertical isothermal hot plate with a high surface-to-ambient temperature difference, *Int. J. Heat Mass Transfer* **25,** 925–934 (1982).
26. R. Cheesewright, Natural convection from a vertical plane surface, Ph.D. Thesis, University of London (1966).
27. C. Y. Warner, Turbulent natural convection in air along a vertical flat plate, Ph.D. Thesis, University of Michigan (1968).
28. E. M. Sparrow and J. L. Gregg, Similar solutions for free convection from a nonisothermal vertical plate, *Trans. ASME* **80,** 379–386 (1958).
29. J. A. B. Wills, The correction of hot-wire readings for proximity to a solid boundary, *J. Fluid Mech.* **12,** 388–396 (1962).
30. K. S. Hebbar and W. L. Melnik, Wall region of a relaxing three-dimensional incompressible turbulent boundary layer, *J. Fluid Mech.* **85,** 33–56 (1978).
31. A. F. Polyakov and S. A. Shindin, Peculiarities of hot-wire measurements of mean velocity and temperature in the wall vicinity, *Lett. Heat Mass Transfer* **5,** 53–58 (1978).
32. J. C. Bhatia, F. Durst and J. Jovanovic, Corrections of hot-wire anemometer measurements near walls, *J. Fluid Mech.* **122,** 411–431 (1982).
33. G. S. H. Lock and F. J. deB. Trotter, Discussion, *J. Heat Transfer* **90,** 494 (1968).
34. W. K. George, Jr. and S. P. Capp, A theory for natural convection turbulent boundary layers next to heated vertical surfaces, *Int. J. Heat Mass Transfer* **22,** 813–826 (1979).
35. ANSI/ASME, Measurement uncertainty, PTC 19.1 (1985).
36. A. A. Townsend, *The Structure of Turbulent Shear Flow*, 2nd Edn. Cambridge University Press, London (1976).
37. M. Miyamoto, H. Kajino, J. Kurima and I. Takanami, Streamwise developments of turbulent characteristics in a vertical free convection boundary layer, *Proc. 18th National Heat Transfer Symposium of Japan*, Sendai, pp. 295–298 (1981).
38. H. P. Kreplin and H. Eckelmann, Behavior of the three fluctuating velocity components in the wall region of a turbulent channel flow, *Physics Fluids* **22**(7), 1233–1239 (1979).
39. M. Hishida and Y. Nagano, Structure of turbulent velocity and temperature fluctuations in fully developed pipe flow, *J. Heat Transfer* **101,** 15–22 (1979).
40. M. Hishida, Y. Nagano and M. Tagawa, Transport processes of heat and momentum in the wall region of turbulent pipe flow, *Proc. 8th Int. Heat Transfer Conf.*, San Francisco, Vol. 3, pp. 925–930 (1986).

CARACTERISTIQUES D'UNE COUCHE LIMITE DE CONVECTION NATURELLE TURBULENTE SUR UNE PLAQUE PLANE VERTICALE

Résumé—Des mesures détaillées sont effectuées en portant attention aux caractéristiques de la région proche de la paroi qui n'a pas été clarifiée quantitativement. On détermine le flux de chaleur et le frottement pariétaux à partir des profils moyens de température et de vitesse, sur des bases théoriques. Ces mesures fournissent des résultats importants concernant la validité de l'analogie conventionnelle entre transferts de chaleur et de quantité de mouvement et du concept de sous-couche visqueuse pour la convection naturelle. On étudie systématiquement le développement de la couche limite turbulente à la fois pour la vitesse moyenne, la température moyenne et les fluctuations de vitesse et de température.

EIGENSCHAFTEN EINER TURBULENTEN GRENZSCHICHT IN NATÜRLICHER KONVEKTION AN EINER VERTIKALEN EBENEN PLATTE

Zusammenfassung—In einer turbulenten natürlichen Konvektionsgrenzschicht wurden detaillierte Hitzdraht-Messungen durchgeführt—unter Berücksichtigung des wandnahen Bereichs, der jedoch nicht qualitativ analysiert wurde. Der Wärmeübergangskoeffizient und die Schubspannung an der Wand werden aus mittleren Temperatur- und Geschwindigkeitsprofilen aufgrund theoretischer Überlegungen ermittelt. Die Messungen führen zu wichtigen Ergebnissen bezüglich der konventionellen Analogie zwischen Wärme- und Impulstransport und der Theorie einer viskosen Unterschicht bei natürlicher Konvektion. Außerdem wird die Entwicklung der turbulenten Grenzschicht in Strömungsrichtung für mittlere Geschwindigkeit und Temperatur und für Geschwindigkeits- und Temperaturschwankungen systematisch untersucht.

ХАРАКТЕРИСТИКИ ТУРБУЛЕНТНОГО ПОГРАНИЧНОГО СЛОЯ У ВЕРТИКАЛЬНОЙ ПЛОСКОЙ ПЛАСТИНЫ ПРИ ЕСТЕСТВЕННОЙ КОНВЕКЦИИ

Аннотация—Проведены детальные термоанемометрические измерения турбулентного естественноконвективного пограничного слоя. Основное внимание обращалось на измерение характеристик теплообмена в пристенной области, которая до настоящего времени детально не рассматривалась. Интенсивность теплопереноса и касательное напряжение на стенке рассчитывались по средним профилям температуры и скорости. Выявлено существование обычной аналогии между тепло-и массопереносом и показана справедливость концепции вязкого подслоя при естественной конвекции. Кроме того, проведено систематическое исследование развития вниз по потоку турбулентного пограничного слоя как по средним значениям скорости и температуры, так и по пульсациям.